

# Curriculum-based Sample Efficient Reinforcement Learning for Robust Stabilization of a Quadrotor

Fausto Mauricio Lagos Suarez<sup>1</sup>, Akshit Saradagi, Vidya Sumathy,  
Shruti Kotpalliwar and George Nikolakopoulos

**Abstract**—This article introduces a curriculum learning approach to develop a reinforcement learning-based robust stabilizing controller for a Quadrotor that meets predefined performance criteria. The learning objective is to achieve desired positions from random initial conditions while adhering to both transient and steady-state performance specifications. This objective is challenging for conventional one-stage end-to-end reinforcement learning, due to the strong coupling between position and orientation dynamics, the complexity in designing and tuning the reward function, and poor sample efficiency, which necessitates substantial computational resources and leads to extended convergence times. To address these challenges, this work decomposes the learning objective into a three-stage curriculum that incrementally increases task complexity. The curriculum begins with learning to achieve stable hovering from a fixed initial condition, followed by progressively introducing randomization in initial positions, orientations and velocities. A novel additive reward function is proposed, to incorporate transient and steady-state performance specifications. The results demonstrate that the Proximal Policy Optimization (PPO)-based curriculum learning approach, coupled with the proposed reward structure, achieves superior performance compared to a single-stage PPO-trained policy with the same reward function, while significantly reducing computational resource requirements and convergence time. The curriculum-trained policy’s performance and robustness are thoroughly validated under random initial conditions and in the presence of disturbances.

## I. INTRODUCTION

In the recent years, artificial intelligence methodologies have significantly influenced the development of controllers for Unmanned Aerial Vehicles (UAVs), with Reinforcement Learning (RL) emerging as a prominent approach, particularly in path planning, navigation, and control of Quadrotors [1][2]. In RL, an agent learns a specific behavior by interacting with its environment, by taking actions, and receiving numeric rewards that indicate the effectiveness of the actions in achieving desired outcomes [3].

RL has proven particularly effective in tackling complex control problems that are challenging for classical system-theoretic approaches [4][5]. This makes RL well-suited for complex learning tasks involving UAVs, where precise modeling of the interaction between the UAV’s nonlinear dynamics and the surrounding aerial flows is highly challenging.

\*This work has been funded by the European Union’s Horizon Europe Research and Innovation Program, under the Grant Agreement No. 101119774 SPEAR.

<sup>1</sup>Fausto Lagos is the corresponding author of the article faulag@ltu.se

The authors are with the Robotics and AI group, in the Department of Computer Science, Electrical and Space Engineering at Luleå University of Technology, Sweden.

However, RL training for UAVs is computationally intensive and time-consuming, underscoring the need for research into sample-efficient RL training methods. Although, using modern GPUs and extreme parallelization in training, millions of time steps (samples) of training can be achieved in minutes [6] [7], it is crucial to investigate the fundamental challenge of sample-efficiency in the training process.

This article addresses the challenge of designing a sample-efficient RL training process to achieve robust stabilization for a Quadrotor starting from random initialization in position, orientation, and velocities. The control objective under consideration and the training methodology aim to advance the use of RL in developing robust, high-accuracy low-level controllers for Quadrotors, contrasting with standard single-stage training approaches commonly used in UAV control, that require several hundred million time steps in one-stage training [8].

Existing literature in RL controller design for Quadrotors has explored diverse aspects, such as reward function design to achieve specific aerial objectives, performance enhancements of RL algorithms, and reduction of computational resources required during training. Notable contributions include [9], which introduced a Bio-inspired Flight Controller (BFC) that mimics natural flying behaviors and [10], which proposed enhancements to the Proximal Policy Optimization (PPO) algorithm for improved learning stability. The work in [4] developed the *GymFC* training environment, demonstrating that RL controllers employing state-of-the-art algorithms such as Deep Deterministic Policy Gradient (DDPG) [11], Trust Region Policy Optimization (TRPO) [12], and PPO [13] can surpass the performance of traditional PID controllers in Quadrotor attitude control. Additionally, [14] introduced an RL-based controller capable of stabilizing a Quadrotor from extreme initial conditions, such as manual tossing. It is worth noting that, in the literature alluded to so far, the sample efficiency of the training process is rarely given any attention.

*Contributions:* This work presents a novel three-stage Curriculum Learning (CL) methodology for training an RL agent to achieve robust stabilization of a Quadrotor, that significantly enhances the sample efficiency of the training process (Section III). To the best of the authors’ knowledge, existing RL methodologies for designing low-level Quadrotor controllers, have not explored curriculum learning, and all reported approaches rely on single-stage training. Our results demonstrate that the proposed three-stage CL approach requires significantly less training time and computational

resources than single-stage training, which fails to achieve the considered learning objectives of robust stabilization, even with extended training periods. The robustness of the proposed curriculum-trained policy are validated through extensive testing with a diverse set of initial conditions and in the presence of disturbances.

## II. PROBLEM FORMULATION

**Quadrotor system.** A Quadrotor is an underactuated aerial system with six degrees-of-freedom (DOF), three translational ( $(x, y, z) \in \mathbb{R}^3$ ) and three rotational ( $\phi, \theta, \psi \in \mathbb{S}^1 \times \mathbb{S}^1 \times \mathbb{S}^1$ ). The Quadrotor is influenced by four control inputs provided by the motors M1-M4. The motors produce upward thrust and the roll, pitch, and yaw rotations necessary for aerial mobility. In this article, a Crazyflie 2.0 (shown in Figure 1) in  $\times$  configuration is considered. Mathematical modeling of the Quadrotor dynamics can be found in [15][16].

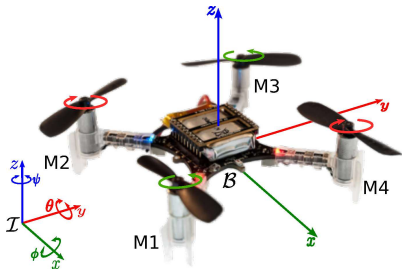


Fig. 1. The Crazyflie Quadrotor.

**Problem statement.** Despite the availability of high-performance computational resources such as Graphics Processing Units (GPUs), training an RL policy to achieve complex control tasks for a Quadrotor, with acceptable performance levels, requires millions of interactions [17] with the training environment. This high demand for interactions makes the training process computationally expensive and time-consuming. To address this challenge, this work looks to propose a methodology for sample-efficient RL training, aimed at achieving robust stabilization of a Quadrotor, from complex initial states and under the influence of external disturbances.

## III. CURRICULUM LEARNING METHODOLOGY

This section introduces a sequenced curriculum, designed to enhance the sample efficiency of the RL training process for Quadrotor control. Curriculum learning involves three key components: sub-task generation, sequencing, and transfer learning. This approach decomposes a complex target task into a series of sub-tasks, progressively transferring knowledge through multiple learning stages until the target is achieved [18].

In this work, a three-stage curriculum is proposed, which is structured using domain knowledge in aerial robotics. In synthesizing a sequence of three sub-tasks, the Quadrotor's under-actuated nature and the coupling between different degrees-of-freedom of a Quadrotor are taken into account.

The training initially focuses on the task of achieving stable hovering from a fixed position. The task difficulty gradually increases in two additional stages, where random initialization in positions/orientations and velocities (both linear and angular) respectively are introduced.

In general, sub-tasks may differ from the final task in terms of state/action space, reward function, or transition dynamics [19] [20]. In this work, we maintain a consistent reward function structure across all sub-tasks, but sequentially expand the domain of initialization of the Quadrotor, thereby altering the environment within the Markov Decision Process (MDP). To develop an RL policy that yields high accuracy, stability, and robustness, while having good sample efficiency in training, we design a compounded reward function (detailed in Section IV-B) that penalizes excessive exploration, instability, and imprecision in reaching the target position and attitude.

The **first sub-task** focuses on achieving a target hover position at  $(x(0), y(0), z(0)) = (0, 0, 1)$ , starting from the fixed position  $(x, y, z) = (0, 0, 0)$ . In this stage, the policy is trained to control the drone to take off and maintain the target position, which essentially involves learning to use the same RPM values for all four motors.

The **second sub-task** increases task complexity by requiring the drone to reach  $(x(0), y(0), z(0)) = (0, 0, 1)$  from random initial positions within a cylinder of 2 meters radius and 2 meters height, and random initial attitudes with roll and pitch angles in a safe range of  $[-15^\circ, 15^\circ]$  and yaw angle in a range of  $[-180^\circ, 180^\circ]$ . This task emphasizes learning the coupling between the three translational degrees of freedom and the roll ( $\phi$ ) and pitch ( $\theta$ ) rotations.

The **third sub-task** further increases difficulty by introducing random initial linear velocities within the range of  $[-1, 1]$  meters per second and angular velocities within the range of  $[-1, 1]$  radians per second, in addition to random initial positions and orientations. Here, the policy learns to manage the motor commands to correct for deviations in position and attitude caused by random initial velocities.

To evaluate the sample efficiency and convergence time of RL training, number of time steps and wall-clock time required to achieve the target task are used as metrics. The proposed curriculum learning is compared against a baseline policy trained in a single stage. The evaluation focuses on the ability of the curriculum-trained policy to meet the final task objectives with reduced training time and enhanced sample efficiency.

## IV. REINFORCEMENT LEARNING SETUP

In the reinforcement learning framework, the control of a Quadrotor is modeled as a Markov Decision Process and represented as a tuple of five elements  $(\mathbb{E}, \pi, \mathbb{A}, \mathbb{S}, \mathbf{R})$ , where  $\mathbb{E}$  is the environment,  $\mathbb{A}$  is the set of actions,  $\mathbb{S}$  and  $\mathbf{R}$  are the current state and rewards returned by the environment, and  $\pi$  is the policy in charge of taking control decisions.

### A. Observation and action spaces

In this work, we consider a 12-dimensional observation space consisting of the position  $[x \ y \ z] \in \mathbb{R}^3$ , the Euler

angles  $[\phi \ \theta \ \psi] \in \mathbb{S}^1 \times \mathbb{S}^1 \times \mathbb{S}^1$ , the linear velocities  $[\dot{x} \ \dot{y} \ \dot{z}] \in \mathbb{R}^3$  and the angular velocities  $[\dot{\phi} \ \dot{\theta} \ \dot{\psi}] \in \mathbb{R}^3$ . The rotor speeds  $R_1, \dots, R_4$  (in RPM) of the propellers constitute the action space. The reinforcement learning policy  $\pi$  maps the observation space to the action space. Although the rotor speeds are an unconventional choice for the action space, this article intends to find an end-to-end policy that directly maps the states to the raw control inputs. The Crazyflie experimental setup considered in this work allows for direct control with the RPMs of the motors (through the PWMs).

### B. Reward shaping

The goal of RL algorithms is to train an agent to obtain the most cumulative reward over time. Although several works in literature (such as [21]) suggest having a simple reward function based on the error in position and velocities, simple rewards leads to sample inefficiency and are not suitable for problems that go beyond hovering. In this paper, a multi-component reward function is designed to consider a wide range of aspects that are crucial for both robust stabilization of a Quadrotor and sample efficiency of the training process. In this article, we propose the following reward function:

$$R(t) = 25 - 20T_e - 100E + 20S - 18w_e, \quad (1)$$

where the individual components are defined below. Although some of the terms are in fact penalties and not rewards, we use the term reward, without loss of generality.

**Target reward ( $T_e$ ):** The target reward is a penalty proportional to the distance between the Quadrotor and the target position ( $T$ ), and the difference between the target yaw and the current yaw. The penalty decreases as the Quadrotor nears the target configuration. The penalty is computed as:

$$T_e = ||[x_T \ y_T \ z_T] - [x \ y \ z]|| + |\psi_T - \psi|, \quad (2)$$

where the target values are indicated through the subscript  $T$ .

**Exploration reward ( $E$ ):** The exploration space for the policy is designed to be a cylinder, centered at the target position ( $T$ ). In each episode, the cylinder's radius is set to the distance between the center and the starting position plus a tolerance  $\delta_R$ , and the height is the target height  $z$  plus a tolerance  $\delta_H$ . This bounded exploration space, along with the truncation conditions for each training episode, help in lowering the overall training time, without compromising the agent's ability to explore adequately. The exploration reward ( $E$ ) is defined as:

$$E = \begin{cases} 1 & d(C, T) > d(i, T) + \delta_R \vee C_z > T_z + \delta_H \\ -0.2 & \text{otherwise} \end{cases}, \quad (3)$$

where  $i$ ,  $C$  and  $T$  refer to the initial, current and target positions respectively.

**Stability reward ( $S$ ):** To ensure that the drone achieves stability at the target position, we provide a positive reward when the drone is within  $\Delta_p$  cm of the target position and the sum-of-squares of the roll and pitch angles are within  $\Delta_a$ .

Otherwise, the drone receives a penalty proportional to the sum of deviations in roll and pitch from zero. The stability reward ( $S$ ) is defined as:

$$S = \begin{cases} 2 & d(C, T) < \Delta_p \wedge \phi^2 + \theta^2 < \Delta_a \\ -(\phi^2 + \theta^2) & \end{cases} \quad (4)$$

The parameter  $\Delta_p$  represents the radius of a tolerance sphere centered at the target position, while  $\Delta_a$  evaluates stability in roll ( $\phi$ ) and pitch ( $\theta$ ) angles.

**Navigation reward ( $w_e$ ):** To ensure smooth navigation from the starting position to the target position, we penalize significant changes in angular velocities. The penalty is proportional to the difference between the angular velocity in the previous time step and the current time step. The navigation reward ( $w_e$ ) is calculated as

$$w_e = \sum_{i=1}^3 (w_{i-1} - w_i)^2, \quad (5)$$

where  $w \in \{\dot{\phi}, \dot{\theta}, \dot{\psi}\}$ . Although we do not impose specific penalties for high roll or pitch angles, we employ truncation conditions to limit extreme behavior, such as when the roll or pitch angle exceeds  $\pm 40^\circ$ .

## V. PROCEDURE FOR SEQUENTIAL TRAINING

In this article, the standard implementation of the Proximal Policy Optimization (PPO) algorithm, considered a state-of-the-art RL algorithm [10], is used to train the curriculum learning policy.

Policy	MlpPolicy	Epochs	10
Learning rate	$3 \times 10^{-4}$	Discount Factor ( $\gamma$ )	0.99
Batch Size	128	Episode Length	5 s

TABLE I  
PARAMETERS FOR THE PPO ALGORITHM.

Parameter	Notation	Value
Mass	$m$	0.027 [Kg]
Arm length	$d$	$39.73 \times 10^{-3}$ [m]
Propeller radius	$p$	$23.1348 \times 10^{-3}$ [m]
Moment of Inertial about $x$ axis	$I_{xx}$	$1.395 \times 10^{-5}$ [Kg $\times$ m <sup>2</sup> ]
Moment of Inertial about $y$ axis	$I_{yy}$	$1.436 \times 10^{-5}$ [Kg $\times$ m <sup>2</sup> ]
Moment of Inertial about $z$ axis	$I_{zz}$	$2.173 \times 10^{-5}$ [Kg $\times$ m <sup>2</sup> ]

TABLE II  
PHYSICAL PARAMETERS OF THE CRAZYFLIE 2.X.

**Training process and simulation engine.** Table I presents the parameters used in the PPO algorithm and Table II presents the physical parameters for Crazyflie 2.x Quadrotor used for simulation. For the training process, we used Gym-PyBullet-Drones [22], a gymnasium [23] environment that uses PyBullet Physics [24] as the physics engine and Stable-Baselines3 [25] as the library of reliable implementations of RL algorithm in PyTorch. *Gym-PyBullet-Drones* was developed to work directly with Crazyflie 2.0 in the  $\times$  and +

configurations, and allows for introducing disturbances into the training environment and during policy testing.

The actor (policy) neural network is an Multi-layered Perceptron (MLP) network [26] with four layers: the first is a layer of 12 inputs (the observation space), the two hidden layers have 64 fully connected nodes with tanh activation functions and the last layer is a four node layer (the action space). The critic (value function) network has the same architecture, except for the last layer which is a one-node layer yielding the output of the value function. Figure 2 shows the architecture of the actor-critic neural networks. The training was executed on a high-performance computing platform with Ubuntu 22.04 and an Intel Core i9 processor with 16 cores CPU and 128 GB RAM, using a NVIDIA GeForce RTX 4090 GPU and Python 3.10. Four parallel environments were used in the training process.

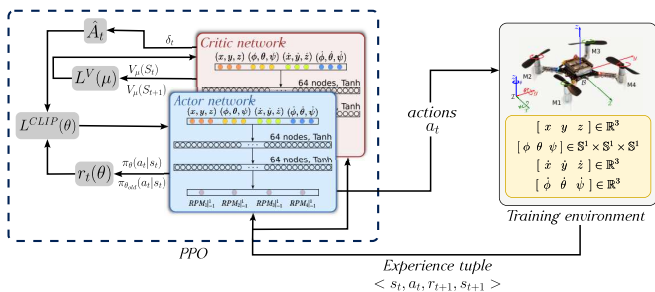


Fig. 2. Reinforcement Learning setup and configuration of the Neural Networks. The RL agent (actor network) interacts with the training environment by generating actions  $a_t$ , based on the current state  $s_t$ , provided by the environment. The actor-network outputs motor RPM values for the Quadrotor’s four motors. The critic network estimates the value function,  $V(s_t)$ , to evaluate the state. The experience tuple  $\langle s_t, a_t, r_{t+1}, s_{t+1} \rangle$  is used to update both actor and critic networks through PPO’s objective function, including the clipped surrogate loss,  $L_{CLIP}(\theta)$ . The state of the Quadrotor includes position, orientation, linear and angular velocities.

To demonstrate the effectiveness of the curriculum learning methodology in achieving the target task and to compare the performance with single-stage training, two agents were trained. The first agent was trained directly on the target task in a single stage (without curriculum learning), and the training process was monitored using the Episode Cumulative Reward (ECR) metric. Using the training setup from section V, after 20 million time steps, which corresponds to more than 6 hours of computation, single-stage training failed to achieve the target task. This can be inferred from the consistently low ECR achieved by single-stage training (Figure 3). The second agent was trained using the three-stage curriculum learning approach proposed in this article. The training process in each stage was monitored, and was terminated once the ECR stabilized for at least one million time steps. Table III presents a comparison of the time steps and wall-clock time required for single-stage training versus curriculum learning. Figure 3 provides a visual comparison of the ECR achieved by the policy trained in one stage versus the policy trained using curriculum learning.

Agent	Time steps	Wall clock
One Stage	20 million	6.8 hours
Sub-task 1	6.2 million	54 minutes
Sub-task 2	6.8 million	57.8 minutes
Sub-task 3	7 million	51 minutes

TABLE III

SAMPLE EFFICIENCY W.R.T TIME STEPS AND WALL CLOCK TIME.

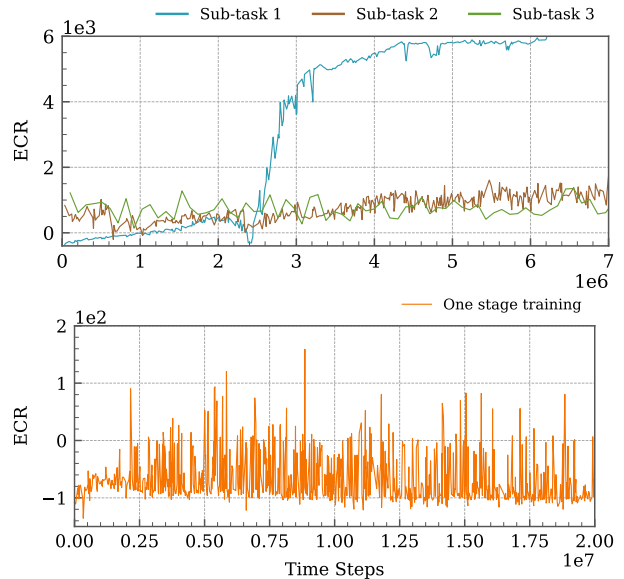
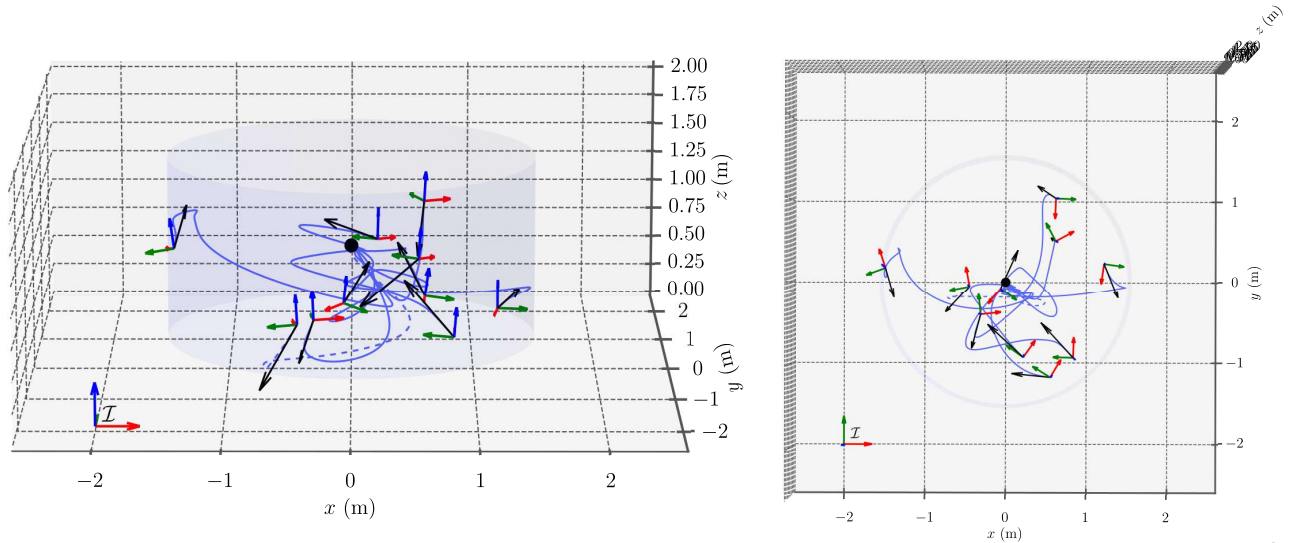


Fig. 3. Episode Cumulative Reward (ECR) comparison between curriculum learning (sub-tasks 1, 2, and 3) and single-stage training (orange). After 20 million time steps (equivalent to 6.8 hours), the single-stage training remains unstable, failing to achieve higher cumulative rewards and demonstrating poor performance on the target task. In contrast, the curriculum learning approach progressively learns to achieve the target task. Sub-task 1 quickly achieves higher cumulative rewards, indicating excellent performance in learning to hover. This knowledge is then effectively transferred to subsequent tasks (Sub-task 2 and 3), which naturally exhibit lower cumulative rewards due to increased task difficulty introduced by random initial conditions and episode truncations.

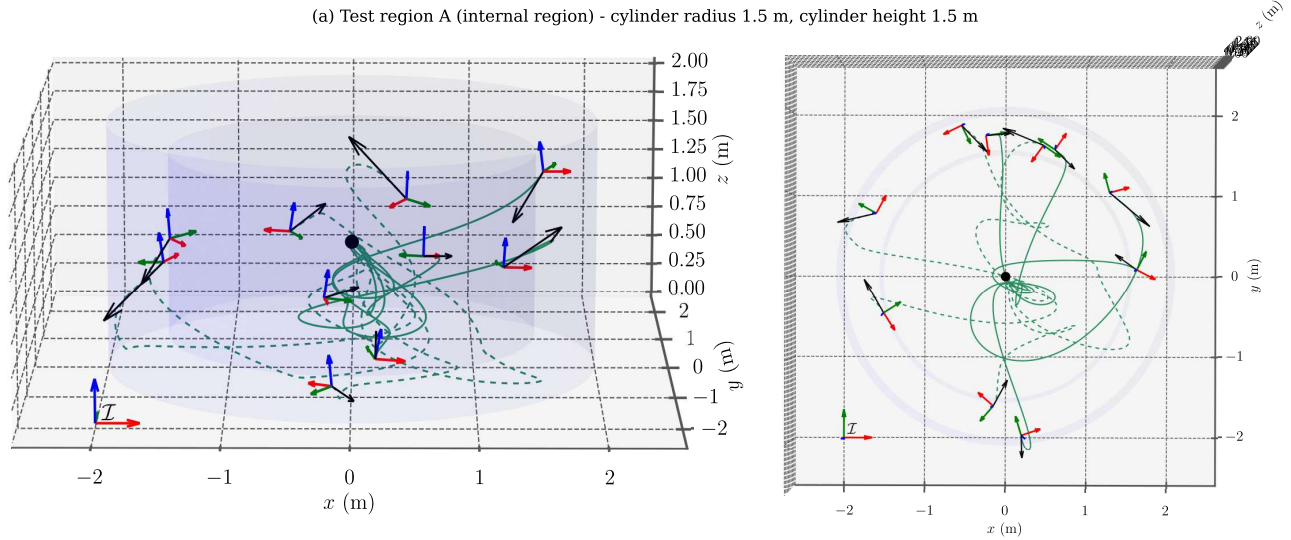
## VI. TESTING OF THE RL POLICY

To evaluate the robustness and stability achieved by the curriculum-trained policy, we design two tests to evaluate: i) the performance of the policy in achieving a target position and orientation, starting from randomized position, orientation, and velocities, and ii) stability in the presence of external disturbances, where the policy’s capacity to recover the desired position and attitude is assessed.

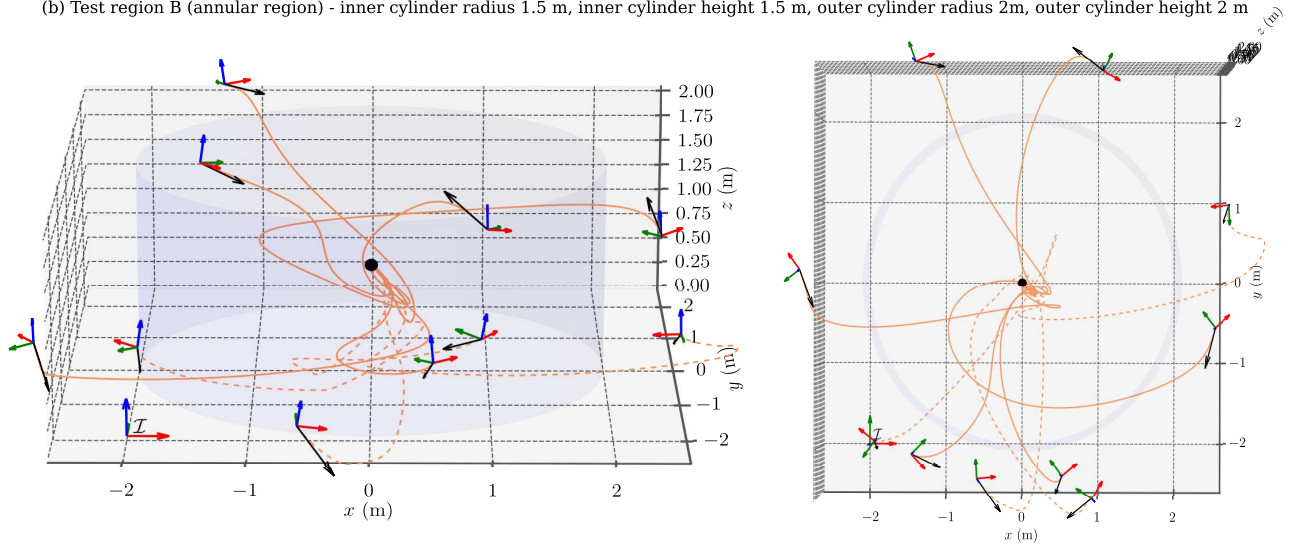
**Robust stabilization:** The performance of the trained policy was evaluated by randomly setting the initial states of the drone and testing its ability to achieve the target configuration  $(x, y, z, \phi, \theta, \psi) = (0, 0, 1, 0, 0, 0)$  and  $(\dot{x}, \dot{y}, \dot{z}, \dot{\phi}, \dot{\theta}, \dot{\psi}) = (0, 0, 0, 0, 0, 0)$ . We conducted 30 trials, each lasting 8 seconds, starting from randomized initial positions, orientations, linear velocities and angular velocities. The 30 initial conditions were split among three regions shown in Figure 4: Test region A, which is a cylinder with radius 1.5 m and height 1.5 m; Test region B, which is an



(a) Test region A (internal region) - cylinder radius 1.5 m, cylinder height 1.5 m



(b) Test region B (annular region) - inner cylinder radius 1.5 m, inner cylinder height 1.5 m, outer cylinder radius 2m, outer cylinder height 2 m



(c) Test region C (outer region) - cylinder radius 2 m, cylinder height 2 m

Fig. 4. Evaluation of the curriculum-trained policy using 30 trials, with initial positions chosen from three regions. At the starting position of the Quadrotor, we use the body coordinate frame to show variations in the initial attitude and a velocity vector (black arrow) to represent the randomized initial linear velocity (the length of the arrow is proportional to the magnitude of the velocity). The Quadrotor is also initialized with random non-zero angular velocities. Solid trajectories represent smooth maneuvers with small transients, while dashed trajectories are used to indicate large transients, where the drone gets close to the ground, to compensate for large unfavorable initial velocities. In all tests, the drone successfully reaches the target position.

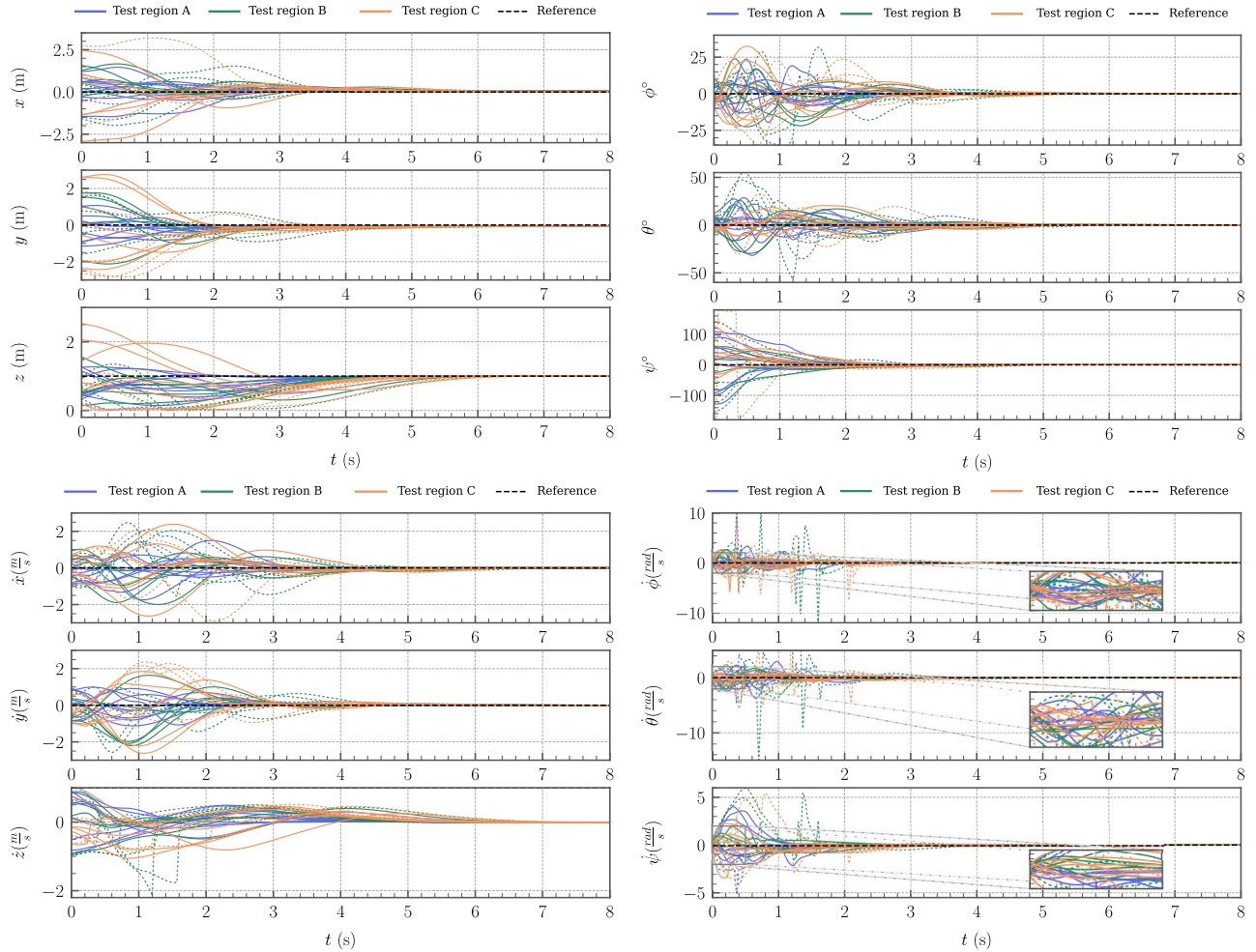


Fig. 5. Performance of the trained policy in achieving robust stabilization from 30 randomized initial conditions. The plots show the evolution of the position (top left), orientation (top right), linear velocities (bottom left), and angular velocities (bottom right) of the Quadrotor. Trajectories with initialization in the three regions A, B and C are shown in different colors: inner cylinder (Region A, blue), annular region (Region B, green), and outer cylinder (Region C, orange). Dashed traces indicate large transients, where the drone reaches close to the ground (seen from the evolution of the  $z$  state), to overcome large initial velocities. The black dashed line represents the reference target values. The curriculum-trained policy consistently drives the system to the target position, from a diverse set of initial states.

annular region with inner radius of 1.5 m, outer radius of 2 m, and height of 2 m; Test region C, which is a cylinder with a radius of 2 m and height of 2 m. For all the trials, the initial roll ( $\phi$ ) and pitch ( $\theta$ ) angles, were randomized in the range  $[-15^\circ, 15^\circ]$  and the yaw ( $\psi$ ) angle in the range of  $[-180^\circ, 180^\circ]$ , the linear velocities were initialized in the range of  $[-1, 1] \frac{m}{s}$  and the angular velocities in the range of  $[-1, 1] \frac{rad}{s}$ . In all scenarios, as can be seen in Figure 4, the drone successfully reached the target position, demonstrating the capability of the curriculum trained policy in robustly stabilizing the Quadrotor at the target position.

In Figure 5, we plot the evolution of the Quadrotor’s position, orientation, linear velocity, and angular velocity from all 30 initial conditions. In most cases, the policy successfully negates the effect of non-zero initial linear and angular velocities and drives the Quadrotor to the target in less than five seconds, with smooth and safe transients. However, in five tests where the initial velocity was excessively high or oriented opposite to the target, the drone exhibited

complex and large transients, bringing the Quadrotor close to the ground, before driving it to the target configuration. In all 30 tests, the curriculum-trained policy consistently guided the drone to the target position with high accuracy, thus achieving robust stabilization of the Quadrotor from a diverse set of initial conditions. Figure 6 presents the motor RPMs generated by the curriculum-trained policy for three representative initial conditions from the regions A, B and C.

**Disturbance rejection:** During a 40-second test run, the drone was subjected to external disturbances, to assess its ability to recover and maintain stability at the target position. Figure 7 demonstrates that the policy successfully recovers from disturbances and returns to the desired position and attitude within approximately three seconds of the disturbances being introduced. The disturbances were applied manually by pushing the drone from its stable position at the target location, using the feature provided by Gym-PyBullet-Drones training and simulation framework.

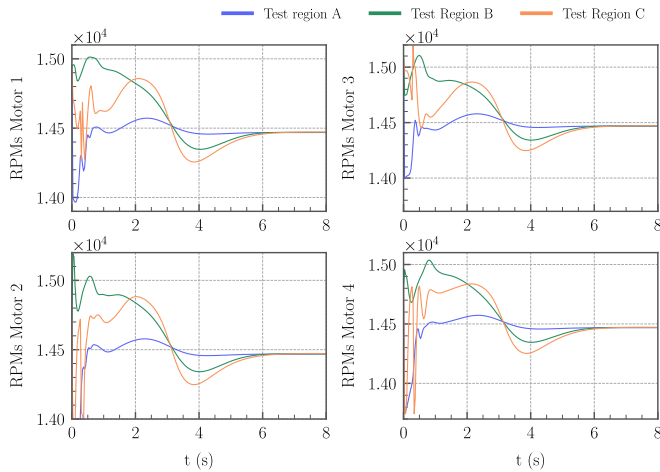


Fig. 6. Motor RPMs generated by the curriculum-trained policy for the four motors of the Crazyflie Quadrotor. The plots show how the motor speeds adjust during flight to stabilize the Quadrotor from three initial conditions corresponding to the regions A, B and C. RPMs of all four motors converge to a common value, as the Quadrotor tends to the target configuration.

## VII. DISCUSSION

**Training process.** The implementation of the PPO algorithm followed the standard implementation provided by the Stable-Baselines3 library. Both the curriculum learning and single-stage training approaches were trained utilizing the same neural network architecture and reward function structure. The evolution of training depicted in Figure 3 clearly shows the effectiveness of curriculum learning in improving sample efficiency. Curriculum learning allows the agent to progressively learn increasingly difficult stabilizing maneuvers, resulting in faster convergence and higher cumulative rewards compared to single-stage training. In contrast, single-stage training approach struggles to achieve the target learning objective for the Quadrotor, with the training remaining unstable and the ECR unable to reach higher reward levels, as can be seen in Figure 3.

**Results.** The results from section VI demonstrate that the proposed curriculum learning approach, combined with the compounded reward function, allows the RL agent to achieve high degree of stability and robustness under complex initial conditions, including random linear and angular velocities. Figure 7 reveals that the trained policy efficiently handles disturbances, recovering the target position and attitude within a few seconds of being perturbed, showcasing the robustness of the curriculum-trained policy. This suggest that the trained agent has the potential to function as a reliable, general purpose low-level controller for Quadrotors, even in challenging operating conditions.

Despite these promising results, there are areas where further improvements can be made. In some instances, particularly when the Quadrotor is initialized at extreme configurations that go beyond those encountered during training, the drone exhibits large transients. This observation points to the need for refining the curriculum learning design to better generalize the agent’s performance across a broader ranger

of initial states. The occasional large transients suggest that additional training stages or more diverse initial conditions could improve the policy’s robustness in extreme scenarios.

Moreover, while the current curriculum-trained policy demonstrated desirable performance in simulation, bridging the gap between simulation and real-world (sim2real) deployment remains a critical challenge. Real-world environments introduce unmodelled dynamics, disturbances and noise that may not be fully captured in the simulation engine. Thus, incorporating specific measures to address sim2real transfer is essential. This would allow the trained policy to be deployed effectively in controlling real Quadrotor systems.

## VIII. CONCLUSION AND FUTURE DIRECTIONS

This work proposed a sample-efficient curriculum learning methodology for efficiently and effectively training a reinforcement learning agent to accomplish robust stabilization for Quadrotors. A compounded reward function was proposed to capture performance specifications related to transient performance, and steady-state accuracy in robust stabilization of a Quadrotor. The performance of the curriculum-trained RL policy was thoroughly tested in a physics based simulator, with different initial conditions and in the presence of disturbances. The results revealed that curriculum training is more sample-efficient than one-stage training, while yielding superior performance. The future work involves automating the curriculum setup and transferring the policy to real drones, thereby closing the simulation-to-reality gap.

## REFERENCES

- [1] A. T. Azar, A. Koubaa, N. Ali Mohamed, H. A. Ibrahim, Z. F. Ibrahim, M. Kazim, A. Ammar, B. Benjdira, A. M. Khamis, I. A. Hameed, and G. Casalino, “Drone Deep Reinforcement Learning: A Review,” *Electronics*, vol. 10, no. 9, p. 999, Jan. 2021, number: 9 Publisher: Multidisciplinary Digital Publishing Institute. [Online]. Available: <https://www.mdpi.com/2079-9292/10/9/999>
- [2] J. Alvarez, A. Belbachir, F. Belbachir, J. Chahal, A. Goudjil, J. Gustave, and A. Öztürk Suri, “Forest Fire Localization: From Reinforcement Learning Exploration to a Dynamic Drone Control,” *Journal of Intelligent & Robotic Systems*, vol. 109, no. 4, p. 83, Nov. 2023. [Online]. Available: <https://doi.org/10.1007/s10846-023-02004-z>
- [3] R. Sutton and A. Barto, *Reinforcement Learning, second edition: An Introduction*, ser. Adaptive Computation and Machine Learning series. MIT Press, 2018. [Online]. Available: <https://books.google.se/books?id=sWV0dWAAQBAJ>
- [4] W. Koch, R. Mancuso, R. West, and A. Bestavros, “Reinforcement Learning for UAV Attitude Control,” *ACM Trans. Cyber-Phys. Syst.*, vol. 3, no. 2, pp. 22:1–22:21, Feb. 2019. [Online]. Available: <https://dl.acm.org/doi/10.1145/3301273>
- [5] L. Antonyshyn and S. Givigi, “Deep Model-Based Reinforcement Learning for Predictive Control of Robotic Systems with Dense and Sparse Rewards,” *Journal of Intelligent & Robotic Systems*, vol. 110, no. 3, p. 100, Jul. 2024. [Online]. Available: <https://doi.org/10.1007/s10846-024-02118-y>
- [6] J. Eschmann, D. Albani, and G. Loianno, “Learning to Fly in Seconds,” Apr. 2024, arXiv:2311.13081 [cs, eess]. [Online]. Available: <http://arxiv.org/abs/2311.13081>
- [7] M. Kulkarni, T. J. L. Forgaard, and K. Alexis, “Aerial Gym – Isaac Gym Simulator for Aerial Robots,” May 2023, arXiv:2305.16510 [cs]. [Online]. Available: <http://arxiv.org/abs/2305.16510>
- [8] B. Xu, F. Gao, C. Yu, R. Zhang, Y. Wu, and Y. Wang, “OmniDrones: An Efficient and Flexible Platform for Reinforcement Learning in Drone Control,” Sep. 2023. [Online]. Available: <https://arxiv.org/abs/2309.12825v1>

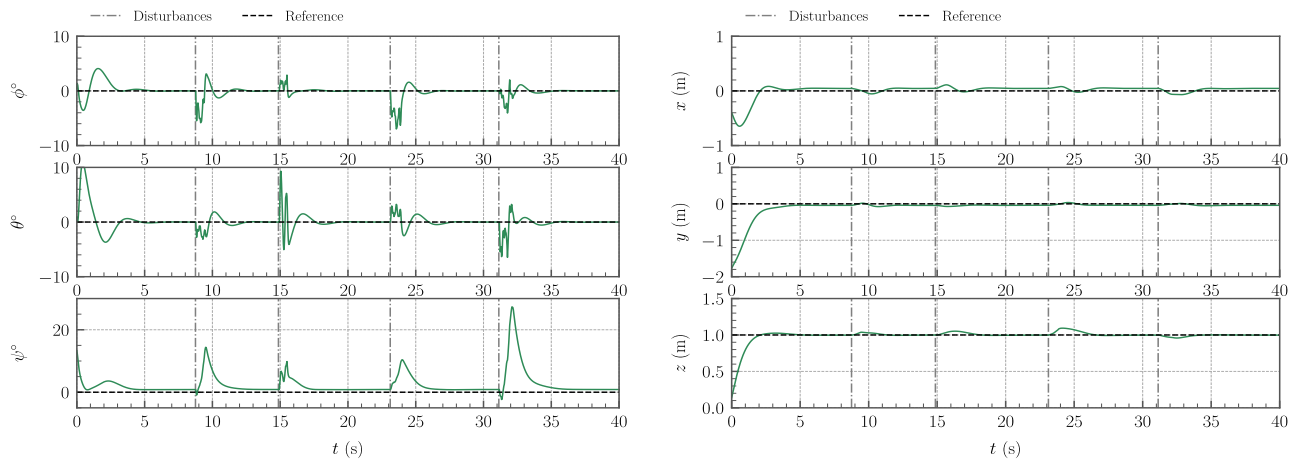


Fig. 7. Performance of the curriculum-trained policy in recovering the target position and attitude when subjected to external disturbances. The plots show the Quadrotor's responses in orientation (left column: roll ( $\phi$ ), pitch ( $\theta$ ), and yaw ( $\psi$ )) and position (right column:  $x$ ,  $y$ , and  $z$ ). The dashed black lines represent the reference values, while the vertical gray dashed lines indicate the moments when disturbances were introduced. The results demonstrate the policy's ability to maintain stability of the target configuration and rapidly recover to the target state, when subjected to external disturbances.

- [9] A. Ramezani Dooraki and D.-J. Lee, "An innovative bio-inspired flight controller for quad-rotor drones: Quad-rotor drone learning to fly using reinforcement learning," *Robotics and Autonomous Systems*, vol. 135, p. 103671, Jan. 2021. [Online]. Available: <https://www.sciencedirect.com/science/article/pii/S092188902030511X>
- [10] W. Xue, H. Wu, H. Ye, and S. Shao, "An Improved Proximal Policy Optimization Method for Low-Level Control of a Quadrotor," *Actuators*, vol. 11, no. 4, p. 105, Apr. 2022, number: 4 Publisher: Multidisciplinary Digital Publishing Institute. [Online]. Available: <https://www.mdpi.com/2076-0825/11/4/105>
- [11] T. P. Lillicrap, J. J. Hunt, A. Pritzel, N. Heess, T. Erez, Y. Tassa, D. Silver, and D. Wierstra, "Continuous control with deep reinforcement learning," Jul. 2019, arXiv:1509.02971 [cs, stat]. [Online]. Available: <http://arxiv.org/abs/1509.02971>
- [12] J. Schulman, S. Levine, P. Moritz, M. I. Jordan, and P. Abbeel, "Trust Region Policy Optimization," Apr. 2017, arXiv:1502.05477 [cs]. [Online]. Available: <http://arxiv.org/abs/1502.05477>
- [13] J. Schulman, F. Wolski, P. Dhariwal, A. Radford, and O. Klimov, "Proximal Policy Optimization Algorithms," Aug. 2017, arXiv:1707.06347 [cs]. [Online]. Available: <http://arxiv.org/abs/1707.06347>
- [14] J. Hwangbo, I. Sa, R. Siegwart, and M. Hutter, "Control of a Quadrotor with Reinforcement Learning," *IEEE Robotics and Automation Letters*, vol. 2, no. 4, pp. 2096–2103, Oct. 2017, arXiv:1707.05110 [cs]. [Online]. Available: <http://arxiv.org/abs/1707.05110>
- [15] R. Beard, "Quadrotor Dynamics and Control Rev 0.1."
- [16] C. Luis and J. L. Ny, "Design of a Trajectory Tracking Controller for a Nanoquadcopter," Aug. 2016, arXiv:1608.05786 [cs]. [Online]. Available: <http://arxiv.org/abs/1608.05786>
- [17] R. Ferede, G. de Croon, C. De Wagter, and D. Izzo, "End-to-end neural network based optimal quadcopter control," *Robotics and Autonomous Systems*, vol. 172, p. 104588, Feb. 2024. [Online]. Available: <https://www.sciencedirect.com/science/article/pii/S0921889023002270>
- [18] S. Narvekar, "Curriculum Learning for Reinforcement Learning Domains: A Framework and Survey," *Journal of Machine Learning Research 21*, Jul. 2020.
- [19] J. Karlsson, "Task Decomposition in Reinforcement Learning." [Online]. Available: <https://aaai.org/papers/0006-ss94-02-006-task-decomposition-in-reinforcement-learning/>
- [20] G. Kwon, B. Kim, and N. K. Kwon, "Reinforcement Learning with Task Decomposition and Task-Specific Reward System for Automation of High-Level Tasks," *Biomimetics*, vol. 9, no. 4, p. 196, Apr. 2024, number: 4 Publisher: Multidisciplinary Digital Publishing Institute. [Online]. Available: <https://www.mdpi.com/2313-7673/9/4/196>
- [21] Z. Jiang and A. F. Lynch, "Quadrotor motion control using deep reinforcement learning," *Journal of Unmanned Vehicle Systems*, vol. 9, no. 4, pp. 234–251, Dec. 2021. [Online]. Available: <https://cdnsiencepub.com/doi/10.1139/juvs-2021-0010>
- [22] "utiasDSL/gym-pybullet-drones" [Online]. Available: <https://github.com/utiasDSL/gym-pybullet-drones>
- [23] "Gymnasium." [Online]. Available: <https://zenodo.org/record/8127025>
- [24] E. C. a. Y. Bai, "PyBullet, a Python module for physics simulation for games, robotics and machine learning," Apr. 2024, original-date: 2011-04-12T18:45:08Z. [Online]. Available: <https://github.com/bulletphysics/bullet3>
- [25] A. Raffin, A. Hill, A. Gleave, A. Kanervisto, M. Ernestus, and N. Dormann, "Stable-baselines3: reliable reinforcement learning implementations," *The Journal of Machine Learning Research*, vol. 22, no. 1, pp. 268:12 348–268:12 355, Jan. 2021.
- [26] M.-C. Popescu, V. E. Balas, L. Perescu-Popescu, and N. Mastorakis, "Multilayer Perceptron and Neural Networks," vol. 8, no. 7, 2009.